

Defective neuroepithelial cell cohesion affects tangential branchiomotor neuron migration in the zebrafish neural tube

Petra Stockinger^{1,2}, Jean-Léon Maître^{1,2} and Carl-Philipp Heisenberg^{1,*}

SUMMARY

Facial branchiomotor neurons (FBMNs) in zebrafish and mouse embryonic hindbrain undergo a characteristic tangential migration from rhombomere (r) 4, where they are born, to r6/7. Cohesion among neuroepithelial cells (NCs) has been suggested to function in FBMN migration by inhibiting FBMNs positioned in the basal neuroepithelium such that they move apically between NCs towards the midline of the neuroepithelium instead of tangentially along the basal side of the neuroepithelium towards r6/7. However, direct experimental evaluation of this hypothesis is still lacking. Here, we have used a combination of biophysical cell adhesion measurements and high-resolution time-lapse microscopy to determine the role of NC cohesion in FBMN migration. We show that reducing NC cohesion by interfering with Cadherin 2 (Cdh2) activity results in FBMNs positioned at the basal side of the neuroepithelium moving apically towards the neural tube midline instead of tangentially towards r6/7. In embryos with strongly reduced NC cohesion, ectopic apical FBMN movement frequently results in fusion of the bilateral FBMN clusters over the apical midline of the neural tube. By contrast, reducing cohesion among FBMNs by interfering with Contactin 2 (Cntn2) expression in these cells has little effect on apical FBMN movement, but reduces the fusion of the bilateral FBMN clusters in embryos with strongly diminished NC cohesion. These data provide direct experimental evidence that NC cohesion functions in tangential FBMN migration by restricting their apical movement.

KEY WORDS: Epithelial cohesion, Hindbrain, Neuronal migration, Zebrafish

INTRODUCTION

Neuronal migration is a fundamental step in the formation of the nervous system. In order to migrate, neurons need to regulate dynamically their adhesion to other cells and the extracellular matrix (ECM). Different families of cell-cell and cell-matrix adhesion molecules (CAMs), such as Integrins, Immunoglobulin CAMs (IgCAMs) and Cadherins, have been implicated in neuronal migration. Among the Cadherins, Cdh2 is widely expressed within the developing nervous system and is required for various processes associated with nervous system development. Cdh2 has also been implicated in neuronal migration by regulating cell-cell and cell-substrate adhesion (Kawauchi et al., 2010; Rieger et al., 2009; Taniguchi et al., 2006). Similar to Cadherins, IgCAMs are thought to play diverse roles in nervous system development (Maness and Schachner, 2007). The IgCAM Cntn2 has been involved in the migration of interneurons in the mouse cortex and facial branchiomotor neurons (FBMNs) in the hindbrain of zebrafish by promoting cell-cell adhesion (Denaxa et al., 2001; Kyriakopoulou et al., 2002; Sittaramane et al., 2009). However, although these findings demonstrate a crucial role of different adhesion molecules for neuronal migration, the function of those molecules in regulating neuronal adhesion, and the role of adhesion in neuronal migration are not yet fully understood.

FBMNs have been used as a model system to study neuronal migration during mouse and zebrafish nervous system development. FBMNs are a subset of the cranial motor neurons in the hindbrain that undergo tangential migration from rhombomere

(r) 4, where they are generated, to r6 and r7 (Fig. 1B), where they will form the facial motor nucleus (Chandrasekhar et al., 1997; Higashijima et al., 2000). Several molecules with diverse functions have been implicated in FBMN migration. Among them are core components of the non-canonical Wnt/Planar cell polarity (Wnt/PCP) pathway (Bingham et al., 2002; Carreira-Barbosa et al., 2003; Jessen et al., 2002; Wada et al., 2005; Wada et al., 2006). The observation that in Wnt/PCP mutant embryos, FBMNs at the basal side of the neuroepithelium exhibit ectopic movements towards the apical midline of the neural tube instead of initiating their characteristic tangential migration to r6/7, has led to the suggestion that Wnt/PCP signaling functions in tangential FBMN migration by restricting their apical movement. It has been speculated further that Wnt/PCP signaling prevents ectopic apical FBMN movement by promoting NC cohesion, indicating a crucial function of NC cohesion in FBMN migration. However, direct evidence that NC cohesion functions in tangential FBMN migration by restricting their apical movement is still lacking.

In this study, we analyze the role of NC cohesion in FBMN migration. Using a combination of cell adhesion measurements and time-lapse imaging, we demonstrate that reducing Cdh2-mediated NC cohesion leads to FBMNs at the basal side of the neuroepithelium moving apically instead of tangentially, frequently leading to an ectopic fusion of the bilateral FBMN clusters over the apical neural tube midline. By contrast, Cntn2-mediated FBMN cohesion has no major function in restricting apical FBMN movement, but is required for the apical fusion of the bilateral FBMN clusters in embryos with strongly reduced NC cohesion.

MATERIALS AND METHODS

Embryo staging and maintenance

Fish maintenance and embryo collection were carried out as described (Westerfield, 2000). Embryos were grown in E3 zebrafish embryo medium at 25°C or 33°C, manipulated in Danieau's buffer and staged according to

¹Institute of Science and Technology Austria, Am Campus 1, A-3400 Klosterneuburg, Austria. ²Max-Planck-Institute of Molecular Cell Biology and Genetics, Pfotenhauerstr. 108, D-01307 Dresden, Germany.

*Author for correspondence (heisenberg@ist.ac.at)

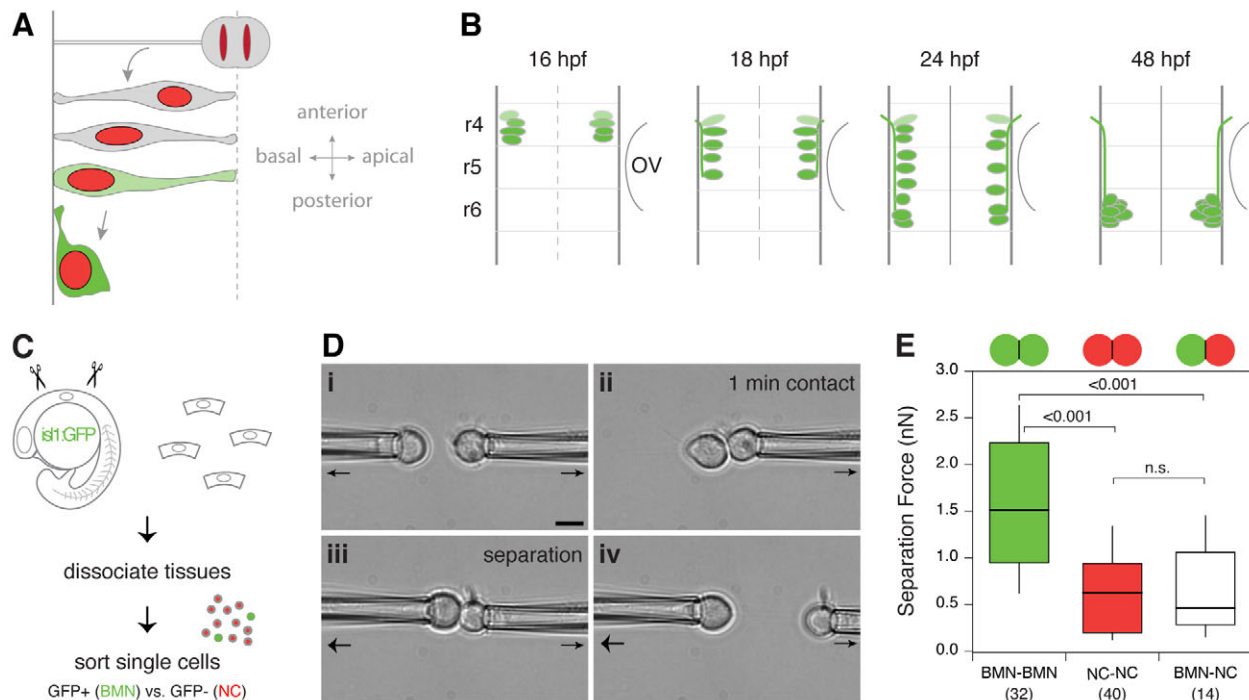


Fig. 1. FBMNs in the zebrafish hindbrain are more cohesive than surrounding NCs. (A) Illustration of FBMN development from neurogenic division to specification (green) and initiation of tangential migration. (B) Schematic of FBMN migration between 16 and 48 hpf. FBMNs form axonal processes, which exit the hindbrain at r4 and later form the facial nerve (adapted from Wada et al., 2005). (C) Schematic of sample preparation. At 18–22 ss, hindbrains from *isl1:GFP* transgenic embryos are dissected and dissociated. Single GFP-expressing BMNs are isolated using fluorescence-activated cell sorting (FACS) and, subsequently, the adhesive properties of cell doublets are measured. (D) Outline of the dual micropipette aspiration assay. Two cells are collected by gentle aspiration in the micropipettes (i) and brought into contact (ii). One cell is held firmly with a holding pressure (thin arrow), whereas the other micropipette applies a separation pressure on the second cell (thick arrow). To measure the force required to separate these cells, the pipettes are pulled apart at stepwise increasing separating pressures (iii) until the level of the separation pressure is sufficient to separate the cells (iv). (E) Box plot of separation forces measured for homotypic adhesion between BMNs (BMN-BMN; green) and NCs (NC-NC; red), and for heterotypic adhesion between BMNs and NCs (BMN-NC; white) after 1 minute of contact time. Box represents the median \pm interquartile range (IQR) and the whiskers extend to $1.5 \times$ IQR. *P* values determined by *t*-test are shown above the brackets. Numbers of measurements are indicated in brackets. OV, otic vesicle; n.s., not significant. Scale bar: 5 μ m.

morphology (Kimmel et al., 1995). The following zebrafish lines and alleles were used: Tg(*isl1:GFP*) (Higashijima et al., 2000) and *cdh2^{fl7}* (Lele et al., 2002). To reduce genetic background variability in our live imaging and in the dual micropipette aspiration assay, we compared Tg(*isl1:GFP*), *cdh2^{fl7}* embryos with either heterozygous (*cdh2^{fl7/+}*) or wild-type (wt) siblings (*cdh2⁺*).

mRNA and morpholino oligonucleotide injections

Cdh2:GFP was generated by sub-cloning full length *cdh2* cDNA fused to GFP into pCS2+ (Jontes et al., 2004). mRNA was synthesized and injected as previously described (Montero et al., 2005). To label cell nuclei, 50–100 pg of H2A-F/Z-mCherry mRNA was injected into the one-cell stage embryo. To visualize Cdh2 localization in the hindbrain (mosaic expression), 25 pg of *cdh2*-GFP mRNA was injected into 32-cell stage embryos. For Cdh2 localization analysis in single cells, a mixture of 50 pg Cdh2-GFP and 50 pg of GPI-mRFP mRNA was injected into one-cell stage embryos. To reduce protein expression, previously described morpholino oligonucleotides (MO) were injected into one-cell stage embryos: *cdh2*, 5'-TCTGTATAAAGAAACCGATAGAGTT-3' (Lele et al., 2002); and *cntn2* (MO1), 5'-CCACACCCAGACCAGACACTTATTT-3' (Liu and Halloran, 2005).

In situ hybridization and antibody staining

Whole-mount in situ hybridization was performed as previously described (Westerfield, 2000). In situ hybridization probes were synthesized from cDNA for *cntn2* (Warren et al., 1999) using a DIG RNA labeling kit

(Roche, Mannheim, Germany). After staining, embryos were embedded in 70% glycerol and photographed on a Zeiss AxioScope using QCapture (QImaging) software. For immunohistochemistry, the embryos were fixed in 4% paraformaldehyde (PFA) at 4°C overnight, washed in 0.1% Tween in PBS and then manually dechorionated. Embryos were first incubated for 5 hours in blocking solution [10% normal goat serum, 0.5–0.8% Triton X-100 in PBS (PBST)] and then overnight at 4°C in blocking solution containing primary antibodies. They were then washed in PBST and incubated overnight at 4°C with secondary antibodies plus Phalloidin/DAPI. Stained embryos were transferred into 70% glycerol in PBST, sectioned using a sharpened tungsten wire and flat-mounted.

For single cell staining, dissociated neuroepithelial cells were allowed to attach onto an uncoated glass-bottomed dish for 30 minutes and were subsequently fixed with 4% PFA for 10 minutes at room temperature. Samples were rinsed with 0.1% Triton X-100 in PBS (PBST-1), blocked for 1 hour in PBS containing 0.1% Triton X-100, 1% DMSO and 10% normal goat serum, and incubated with primary antibody in blocking solution for 1 hour at room temperature. After several washes with PBST-1, samples were incubated in secondary antibody for 30 minutes and rinsed several times with PBST-1 before imaging. Sample imaging was performed on a Zeiss or Leica confocal microscope using a Plan-Apochromat 40 \times /1.2 W or 63 \times /1.2 W objective. The following primary antibodies and dilutions were used: mouse anti- β -catenin (Sigma, 1:200), rabbit anti-Cdh2 (1:200), rabbit anti-Fibronectin (Sigma, 1:200), mouse anti-GFP (mAb3E6) (Invitrogen, 1:20), rabbit anti-GFP (Invitrogen, 1:1000), anti-phosphohistone H3 (Upstate Biotech, 1:200), mouse anti-HuC/D protein (16A11)

(Invitrogen, 1:500), rabbit anti-Laminin (Sigma, 1:200), rabbit anti-nPKC (C-20) (Santa Cruz, 1:200), mouse anti-acetylated α -tubulin (6-11B-1) (Sigma, 1:1000), mouse anti- γ -tubulin (Sigma, 1:1000) and mouse anti-ZO-1 (Invitrogen, 1:200). For secondary antibodies, Alexa 488- and Cy5-coupled anti-mouse and anti-rabbit IgGs (Alexa 488: Molecular Probes, 1:500; Cy5: Jackson ImmunoResearch, 1:400) were used. Rhodamine-phalloidin (Invitrogen, 1:100) was used for F-actin staining and DAPI (Invitrogen, 1:100) was used for nuclear labeling.

Production of anti-Cdh2 antibody

A polyclonal antibody against the zebrafish Cdh2 protein was purified from rabbits, which were immunized with the synthetic peptide CNAGPYAFELPNRPSDIRRNWTL (NeoMPS) directed against cadherin domain 5 (aa620-641).

Two-photon excitation timelapse microscopy

Embryos were manually dechorionated in Danieau's buffer containing 0.08% Tricaine and mounted in 1% low-melting-point agarose prior to imaging; time-lapse, multiple focal plane (4D) microscopy was performed at 28.5°C. Imaging of 6-18 somite stage (ss) embryos was performed on an upright LaVision Biotec TrimScope using a Zeiss C-Achroplan 32 \times /0.85 W objective. Images of 18-22 ss embryos were acquired on an upright Zeiss LSM 7 MP system using a Plan-Apochromat 40 \times /1.2 W objective. For dual color imaging, GFP and mCherry were simultaneously excited using 960-980 nm wavelengths. Movies were processed using Imaris (Bitplane) software.

Image quantification and movement analysis

For FBMN movement analysis, the acquired *z*-stacks were volume rendered in 3D over time using Imaris software (Bitplane). Tissue movements were corrected for by employing the spot recognition function to detect cell nuclei of floor plate cells and, subsequently, the drift correction function. For movement analysis of FBMNs, their nuclei were detected and manually tracked over time in 3D (*x,y,z*). Cell migration paths, instantaneous speed and tangential displacement speed (total *y*-displacement divided by time) were calculated using Microsoft Excel software. Quantification of microtubule organizing center (MTOC) position, FBMN cluster distance and cell-cell contact length were performed using measurement tools in Imaris and ImageJ. Statistical analysis was carried out using either an unpaired two-tailed Student's *t*-test with no equal variance assumption or a two-sample Kolmogorov-Smirnov test. Plots were created using Excel (Microsoft), IgorPro software (Wavemetrics) or Prism (GraphPad).

Dual micropipette aspiration assay

The dual micropipette aspiration assay was performed as described previously (Daoudi et al., 2004). To isolate cells, hindbrains of *isl1*:GFP transgenic embryos at 18-22 ss were dissected in DMEM/F12 (Invitrogen) and dissociated for 8 minutes using 0.05% Trypsin-EDTA (Invitrogen). GFP-expressing branchiomotor neurons (BMNs) were then sorted from neuroepithelial cells using a BD FACSAria III cell sorter. Cells were kept in DMEM/F12 containing 10% fetal bovine serum (FBS, Invitrogen) at 25°C for up to 3 hours after sorting and manipulated with two micropipettes, each held by a micromanipulator connected to a microfluidic pump (Fluigent). Micropipettes with an internal diameter of 2.5-5.5 μ m were pulled (model P-97; Sutter Instrument), cut and fire-polished. Cells were imaged with an inverted epifluorescence microscope (Zeiss) equipped with a 40 \times objective (Zeiss LD PlanNeoFluar 0.6 numerical aperture Ph2 Korr) and a cooled charge-coupled device CoolSnap HQ (Photometrics). Images were acquired using Metamorph software.

RESULTS

FBMNs are more cohesive than surrounding NCs

In order to address the function of NC cohesion for FBMN migration, we first characterized the adhesive properties of FBMNs and surrounding NCs during FBMN migration. To measure FBMN and NC adhesion, we isolated individual BMNs and NCs from the hindbrain of *isl1*:GFP transgenic embryos at the 18-22 ss, which

express GFP in all BMNs specified at this stage [18-19.5 hours post-fertilization (hpf); Fig. 1C]. Given that a large proportion of BMNs at the 18-22 ss are FBMNs, we assume that our BMN adhesion measurements reveal FBMN adhesion. We determined the forces required to separate homotypic (BMN-BMN; NC-NC) and heterotypic (BMN-NC) cell pairs using a dual micropipette aspiration assay (Fig. 1D; see Movie 1 and Fig. S1 in the supplementary material). We found that the average separation force (SF) for homotypic BMN pairs at 1 minute (min) contact time was significantly higher than for NC pairs (SF_{BMN}=1.55 nN, SF_{NC}=0.70 nN, *P*<0.001; Fig. 1E), indicating that BMNs are more cohesive than NCs. The SF force for heterotypic cell pairs was comparable to the SF force of homotypic NC pairs (SF_{BMN-NC}=0.64 nN; Fig. 1E), suggesting that adhesion between BMNs and NCs is similar to the cohesion among NCs. Taken together, these findings suggest that in wt embryos, FBMNs are more cohesive than their surrounding NCs and that the heterotypic adhesion between FBMNs and NCs is comparable to homotypic adhesion between NCs.

Cdh2 is required for both NC and FBMN cohesion

Cdh2 has previously been shown to be expressed in the developing zebrafish central nervous system and to be required for neuroepithelial integrity (Lele et al., 2002). We therefore reasoned that interfering with Cdh2 expression might be a suitable approach to reduce NC cohesion and then analyze resulting alterations in FBMN behavior. To investigate whether Cdh2 is involved in NC and/or FBMN adhesion, we first analyzed Cdh2 expression and localization at the 18 ss. Consistent with previous findings (Harrington et al., 2007), *cdh2* mRNA was found to be expressed ubiquitously within the developing hindbrain (data not shown). To analyze the subcellular localization of Cdh2 protein, we generated a polyclonal antibody directed against Cdh2 and performed Cdh2 antibody staining on hindbrain tissues. Similar to *cdh2* mRNA, Cdh2 protein was uniformly expressed within the hindbrain (Fig. 2A,A'). Cdh2 was found at the plasma membrane of both FBMNs and NCs in punctate accumulations that were found particularly at the apical side of these cells facing the forming hindbrain ventricle (Fig. 2B,B'). No obvious difference in Cdh2 expression and/or localization was detectable between FBMNs and NCs (Fig. 2B,B').

To determine the function of Cdh2 in NC and/or FBMN adhesion, we isolated individual BMNs and NCs from the hindbrain of *isl1*:GFP transgenic *cdh2* mutant embryos (Lele et al., 2002) and measured their homotypic and heterotypic adhesion. Whereas homotypic adhesion of *cdh2* mutant NCs was nearly completely abolished (SF_{NC}=0.30 nN, *P*<0.0013; Fig. 2C), BMNs from *cdh2* mutants retained some recognizable, albeit strongly reduced, level of homotypic adhesion (SF_{BMN}=0.48 nN, *P*<0.001; Fig. 2C). Heterotypic adhesion between BMNs and NCs from *cdh2* mutants (SF_{BMN-NC}=0.57 nN; Fig. 2C) was indistinguishable from heterotypic adhesion in wt cells, and comparable to the reduced homotypic adhesion level of *cdh2* mutant BMNs. These findings suggest that Cdh2 is required for most of NC cohesion and for some, but not all, FBMN cohesion, but has no effect on heterotypic adhesion between NCs and FBMNs.

Lowering NC and FBMN cohesion causes FBMNs to move apically instead of tangentially

To determine whether the reduction in NC and FBMN cohesion observed in *cdh2* mutant embryos results in recognizable defects in FBMN morphogenesis, we analyzed FBMN movement in the hindbrain of *cdh2* mutants and embryos injected with different

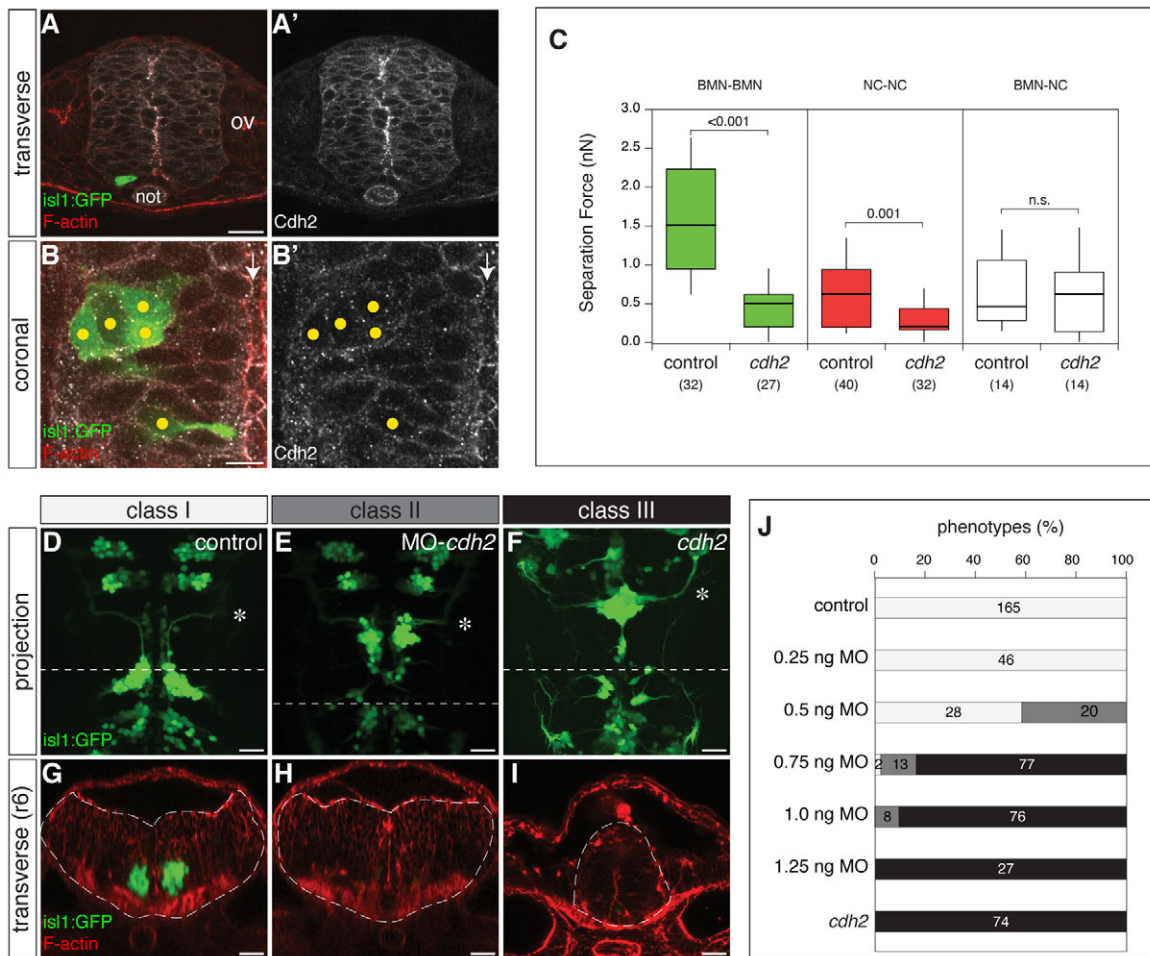


Fig. 2. Reduced NC and FBMN cohesion in *cdh2* mutants is accompanied by defects in FBMN morphogenesis. (A-B') Immunofluorescence staining of Cdh2 protein of *isl1:GFP* transgenic embryos at 18 ss. Transverse sections of the neural tube at the level of r5 (A,A') and higher magnification of a coronal section at the level of r4 (B,B'). White arrows indicate the position of the neural tube midline and yellow dots the position of FBMNs. (C) Box plot of homotypic BMN-BMN (green), homotypic NC-NC (red) and heterotypic BMN-NC (white) separation force measurements of control and *cdh2* mutant cells. Box represents the median \pm interquartile range (IQR) and the whiskers extend to $1.5 \times$ IQR. *P* values determined by *t*-test are shown above the brackets. Numbers of measurements are indicated in brackets. (D-F) Reduction of Cdh2 levels affects FBMN migration. Whereas in wt embryos FBMN are located within r6 and their axonal processes exit the hindbrain at r4 (D), FBMN are mainly localized within r4 in *cdh2* morphant (E) and mutant (F) embryos at 48 hpf. Asterisks indicate FBMN axonal exit point at r4. Dashed lines in D-F indicate level of transverse section shown in G-I. Injecting suboptimal doses of *cdh2* MO leads to intermediate phenotypes with reduced FBMN migration, but normal neural tube morphogenesis (H). In G-I, dashed lines indicate outline of neural tube. (J) Quantification of *cdh2* mutant and morphant phenotypes. Different concentrations of *cdh2* MO were injected into the Tg(*isl1:GFP*) embryos, and changes in FBMN migration and hindbrain morphogenesis were scored at 36-48 hpf (phenotypic classes I-III). Numbers of scored embryos for each phenotype are shown within the bar. not, notochord; OV, otic vesicle; n.s., not significant. Scale bars: 20 μ m in A; 10 μ m in B; 20 μ m in D-I.

amounts of a previously published *cdh2* MO (Lele et al., 2002). In both *cdh2* mutant and morphant embryos, FBMNs were normally specified in r4 but failed to exit r4 and migrate tangentially towards r6/7 (Fig. 2E,F). The FBMN migration defect in *cdh2* mutant embryos was accompanied by severe defects in the general epithelial organization of dorsal parts of the forming hindbrain (Fig. 2I,J; class III phenotype). By contrast, injection of suboptimal concentrations of *cdh2* MO caused intermediate (hypomorphic) phenotypes in which FBMN migration was defective, but the general epithelial organization of the developing hindbrain appeared to be unaffected at 48 hpf (Fig. 2H,J; class II phenotype).

To determine whether there are defects in NC and/or FBMN morphogenesis, other than reduced cohesion (Fig. 2C), which might be responsible for the FBMN migration defect in *cdh2*

mutant embryos, we analyzed overall epithelial organization (Fig. 3A,B), junction formation (Fig. 3C,D), cell polarization (Fig. 3E,F; see Fig. S2 in the supplementary material), ECM deposition (Fig. 3G-J), ciliogenesis (Fig. 3K,L), mitosis (Fig. 3M,N) and neuronal specification (Fig. 3O,P). Although many of these features were clearly affected in dorsal regions of the hindbrain in *cdh2* mutant embryos, no obvious defects were observed within the ventral hindbrain where FBMNs are specified and migrate (Fig. 3A,B). The only clear alteration recognizable in *cdh2* mutant embryos was an $\sim 25\%$ (wt=89 \pm 1 μ m; *cdh2*=66 \pm 0.8 μ m) reduction in the width of the ventral neural tube at the time of FBMN migration (Fig. 3). However, this reduction did not lead to changes in the relative position of other structures within the ventral neural tube, such as the position of HuC/D-positive primary neurons (except FBMNs,

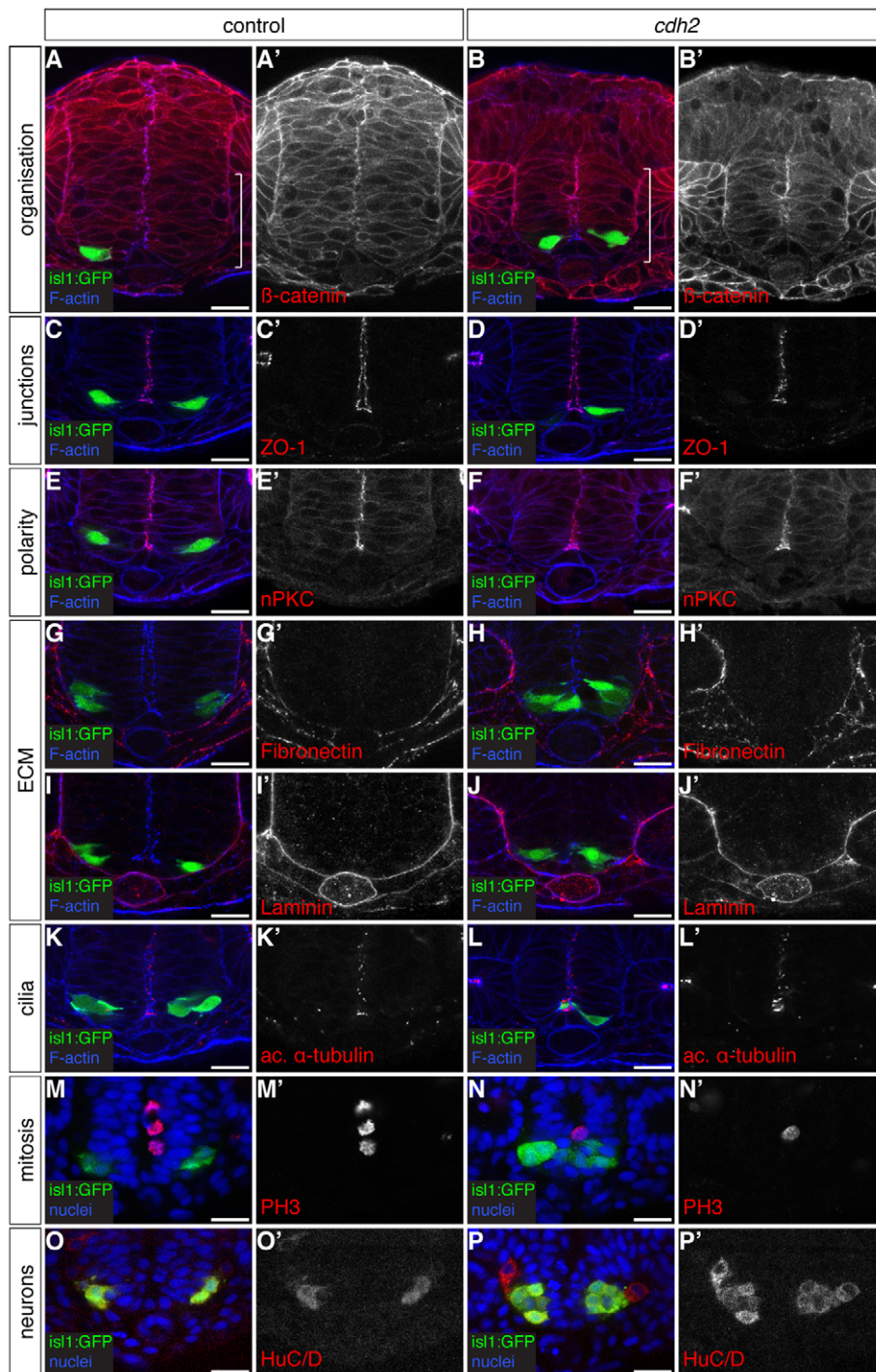


Fig. 3. Reduced NC cohesion in *cdh2* mutants does not affect ventral neural tube morphogenesis. (A-P') Confocal images of wt and *cdh2* mutant transgenic *isl1:GFP* embryos at 18 ss immunolabeled with antibodies against β -catenin (A-B'), tight junction protein ZO-1 (C-D'), apical protein nPKC (E-F'), extracellular matrix components Fibronectin (G-H') and Laminin (I-J'), acetylated α -tubulin (K-L'), phospho-Histone H3 (M-N') and HuC/D (O-P'). Shown are transverse sections with GFP in green, F-actin or DAPI-labeled nuclei in blue and antibody labeling in red/white. Brackets indicate ventral part of the neural tube (A,B). Scale bars: 20 μ m.

see below; see Fig. S3 in the supplementary material), suggesting that the general architecture of the ventral neural tube at stages of FBMN migration remains largely intact in *cdh2* mutant embryos.

However, in contrast to this seemingly normal neuroepithelial architecture and polarity in *cdh2* mutants, the two bilateral FBMN clusters, which are normally positioned in the basolateral neuroepithelium of r4, were displaced towards the apical midline of the neural tube in *cdh2* mutant embryos (see Fig. S2E in the supplementary material). In *cdh2* mutant embryos showing a strong phenotype, the apically displaced bilateral FBMN clusters even

fused over the apical neural tube midline and partially segregated from the surrounding neuroepithelium (see Fig. S3D in the supplementary material).

To elucidate the basis of the FBMN migration and localization defects in *cdh2* mutant embryos, we recorded high-resolution movies of FBMN movements in wt and *cdh2* mutant *isl1:GFP* transgenic embryos using a two-photon laser scanning microscope. To determine the position of FBMNs prior to migration, we recorded movies of 6-18 ss embryos (Fig. 4A-C,E-G; see Movies 2 and 3 in the supplementary material) and (back) tracked the

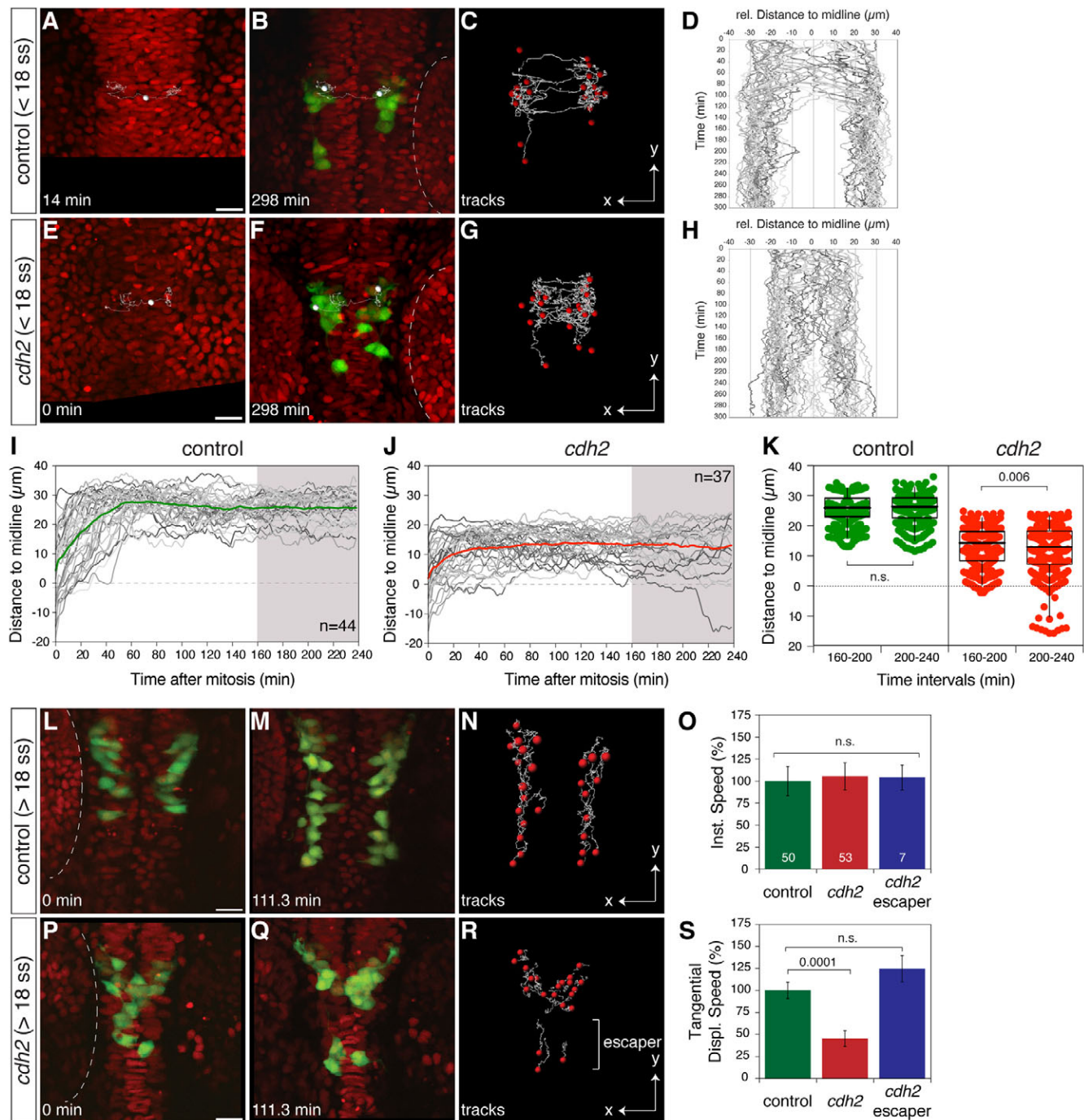


Fig. 4. *Cdh2* is required for FBMN positioning/movements. (A-C,E-G) Live imaging of FBMN movements in wt and *cdh2* mutant embryos. FBMNs are visualized using the *isl1*:GFP transgenic line and all nuclei are labeled with H2A-mCherry. Spots indicate position of nuclei of FBMN precursors directly after neurogenic division (~6 ss embryo; A,E) and 5 hours later (~18 ss embryo; B,F). The tracks in C,G delineate all FBMN movements in embryos from 6-18 ss (red spots mark their final position). Dashed lines in B,F indicate outline of otic vesicle. (D,H) Distances of FBMN nuclei relative to the midline (apicobasal positioning within the neuroepithelium; midline=0 μm) as a function of time in control (D) and *cdh2* mutant (H) embryos (0 min corresponds to beginning of movies). (I,J) Distances of FBMN nuclei relative to the midline (0 μm) as a function of time after their neurogenic division (0 min) in control (I) and *cdh2* mutant (J) embryos. Colored lines are mean distances. n, number of tracks analyzed. (K) FBMN distances relative to the midline (0 μm) between 160-200 and 200-240 min after neurogenic division in control and *cdh2* mutant embryos. Box represents the median \pm interquartile range (IQR) and the whiskers extend to 2.5 and 97.5 percentiles. P values determined by two-sampled Kolmogorov-Smirnov test are shown. (L-N,P-R) Live imaging of FBMN migration in wt and *cdh2* mutant embryos starting around 18 ss. Tracks represent movement of FBMN nuclei and their final positions are indicated by a red spot (N,R). Dashed lines in L,P indicate outline of otic vesicle. (O,S) Normalized average instantaneous speed (O) and tangential displacement speed (S) for all FBMNs in control and *cdh2* mutants, and for FBMNs that manage to exit r4 ('escapers') in *cdh2* mutants. Graphs represent mean \pm s.d. (O) or mean \pm s.e.m. (S). P values determined by t-test are shown above the brackets. n.s., not significant. Scale bars: 20 μm .

movement of FBMN nuclei (marked with H2A-mCherry) from the initiation of FBMN migration to their birth (Fig. 4D,H). Initially, the nuclei of both wt and *cdh2* mutant FBMN precursors moved from the midline where they are born towards the basal side of the neuroepithelium (Fig. 4I,J). However, whereas control FBMNs remained at the basal side of the neuroepithelium until the start of their migration around 200 min after their final mitosis, *cdh2* mutant FBMNs frequently moved back towards the apical midline of the neural tube (Fig. 4J). This observation was confirmed by analyzing changes in the distance of FBMNs to the apical midline in wt and *cdh2* mutant embryos between 160 and 240 min after their final mitosis, revealing significant changes in *cdh2* mutant embryos that were not detectable in wt embryos ($wt_{160-200}=25.7\pm 4.5$ μm ; $wt_{200-240}=25.7\pm 4.8$; $cdh2_{160-200}=13.1\pm 6.1$; $cdh2_{200-240}=12.0\pm 8.1$; Fig. 4K). Importantly, these changes in apicobasal positioning of FBMNs in *cdh2* mutant embryos were not accompanied by obvious alterations in FBMN motility and/or protrusive activity (Fig. 4O; see Movie 8 in the supplementary material), suggesting that the changes of FBMN positioning in *cdh2* mutants are not just a secondary consequence of defective FBMN motility in *cdh2* mutant embryos.

To test how the defective basal localization of FBMNs in *cdh2* mutant embryos relates to their tangential migration, we recorded movies of 18–22 ss embryos. Whereas FBMNs migrated along the basal side of the neuroepithelium from r4 to r6 in wt embryos (Fig. 4L–N; see Movie 4 in the supplementary material), FBMNs moved apically in between NCs and failed to exit r4 in *cdh2* mutants (Fig. 4P–R; see Movie 5 in the supplementary material). Although this resulted in significantly reduced tangential migration of FBMNs in *cdh2* mutant embryos [displacement speed (DS)_{control}= 0.15 ± 0.1 $\mu\text{m}/\text{min}$, DS_{cdh2} = 0.07 ± 0.1 $\mu\text{m}/\text{min}$], a small proportion of FBMNs, which still managed to exit r4 ('escapers'), migrated caudally at a similar speed to their wt counterparts (DS_{esc} = 0.18 ± 0.06 $\mu\text{m}/\text{min}$; Fig. 4S). This suggests that Cdh2 is required for movement direction of FBMNs in r4, but is not required for FBMN motility per se. It also raises the possibility that FBMNs in *cdh2* mutants fail to translocate from r4 to r6/7 because they move apically within r4 instead of tangentially toward r6/7.

Taken together, the analysis of *cdh2* mutant embryos suggests that NC and/or FBMN cohesion functions in FBMN migration by controlling the direction of FBMN movement within the neuroepithelium.

Lowering Cntn2-mediated FBMN cohesion has no effect on apical-basal FBMN movement

To determine which of the observed changes in cell cohesion is causing the FBMN morphogenesis phenotype in *cdh2* mutants, we attempted to lower cohesion of FBMNs specifically by reducing the expression of Contactin 2 (Cntn2), which has previously been shown to be expressed exclusively in FBMNs and to be required for FBMN morphogenesis (see Fig. S4 in the supplementary material) (Sittaramane et al., 2009). In order to achieve this, we isolated individual BMNs and NCs from *isl1*:GFP transgenic embryos that were injected with a previously published *cntn2* MO (Liu and Halloran, 2005) and measured their homotypic and heterotypic adhesion. Homotypic adhesion of *cntn2* morphant BMNs was reduced, but not completely abolished (SF_{BMN} = 1.14 nN, $P<0.05$; Fig. 5A). By contrast, homotypic adhesion of *cntn2* morphant NCs remained unchanged (SF_{NC} = 0.62 nN; Fig. 5A), as expected from the apparent lack of *cntn2* expression in these cells (Chandrasekhar et al., 1997). Similar to *cdh2* cells, heterotypic adhesion between BMNs and NCs (SF_{BMN-NC} = 1.23 nN; Fig. 5A)

was comparable to the reduced homotypic adhesion level of *cntn2* mutant BMNs and slightly higher than heterotypic adhesion in wt embryos. This suggests that knocking down Cntn2 expression lowers FBMN cohesion specifically and also slightly increases heterotypic adhesion between FBMNs and NCs.

To investigate whether reduced FBMN cohesion and increased FBMN-to-NC adhesion in *cntn2* morphant embryos causes ectopic apical movement of FBMNs, similar to the situation in *cdh2* mutants, we recorded high-resolution movies of FBMN movements in *cntn2* morphant embryos (Fig. 6A–C; see Movie 6 in the supplementary material). Consistent with previous observations (Sittaramane et al., 2009), we found that, similar to the situation in *cdh2* mutant embryos (Fig. 4J), FBMNs in *cntn2* morphant embryos normally moved from the midline of r4, where they are born, towards the basal side of the neuroepithelium (data not shown), but that subsequent tangential migration towards r6/7 was reduced ($DS_{control}$ = 0.21 ± 0.11 $\mu\text{m}/\text{min}$, DS_{cntn2} = 0.13 ± 0.1 $\mu\text{m}/\text{min}$; Fig. 6A–C,H). However, in contrast to the situation in *cdh2* mutants, FBMNs in *cntn2* morphant embryos, although still appearing generally protrusive and motile (Fig. 6A,D), did not move from the basal side of the neuroepithelium apically toward the neural tube midline, but instead segregated from the basal side of the neural tube at later developmental stages (Fig. 5E). Basal segregation of FBMNs was accompanied by defects in basal lamina formation (Laminin deposition) in *cntn2* morphant embryos (Fig. 6M,M'), suggesting that the outer surface of the hindbrain functions as a barrier for FBMN migration (Grant and Moens, 2010). Other features of the developing hindbrain, such as cell polarization and junction formation, appeared to be unaffected in *cntn2* morphant embryos (Fig. 5F–K).

These findings indicate that reducing FBMN cohesion and/or increasing FBMN-to-NC adhesion in *cntn2* morphant embryos is not sufficient to trigger ectopic apical FBMN movement. It further suggests that ectopic apical FBMN movement in *cdh2* mutant embryos must, at least partially, be due to lowered NC cohesion.

Cntn2-mediated FBMN cohesion is required for fusion of the bilateral FBMN clusters in *cdh2* mutants

Although the analysis of *cntn2* morphant embryos suggests that changing FBMN cohesion and FBMN-to-NC adhesion alone is not sufficient to trigger ectopic apical FBMN movement, it is still possible that FBMN cohesion and/or FBMN-to-NC adhesion can modulate the activity of NC cohesion in controlling FBMN morphogenesis. To test this possibility, we tried to lower FBMN cohesion in *cdh2* mutants by generating double mutant/morphant *cdh2/cntn2* embryos. We injected *cntn2* MO into *isl1*:GFP transgenic *cdh2* mutants and measured the adhesion of BMNs and NCs. Homotypic adhesion of double mutant/morphant NCs was comparable to homotypic adhesion of *cdh2* single mutant NCs (SF_{NC} = 0.37 nN; Fig. 5A), confirming our previous observation that Cntn2 has no major role in NC cohesion (Fig. 5A). By contrast, homotypic adhesion of double mutant/morphant BMNs was nearly completely abolished (SF_{BMN} = 0.26 nN; Fig. 5A), similar to the homotypic adhesion observed between NCs from *cdh2* single and *cdh2/cntn2* double mutant embryos. Heterotypic adhesion strength between double mutant/morphant BMNs and NCs was similar to that of homotypic BMN and NC adhesion (SF_{BMN-NC} = 0.25 nN; Fig. 5A) and was reduced compared with heterotypic adhesion in wt cells.

To investigate whether the enhanced reduction in FBMN cohesion and/or FBMN-to-NC adhesion in *cdh2/cntn2* double mutants compared with *cdh2* single mutant embryos further alters

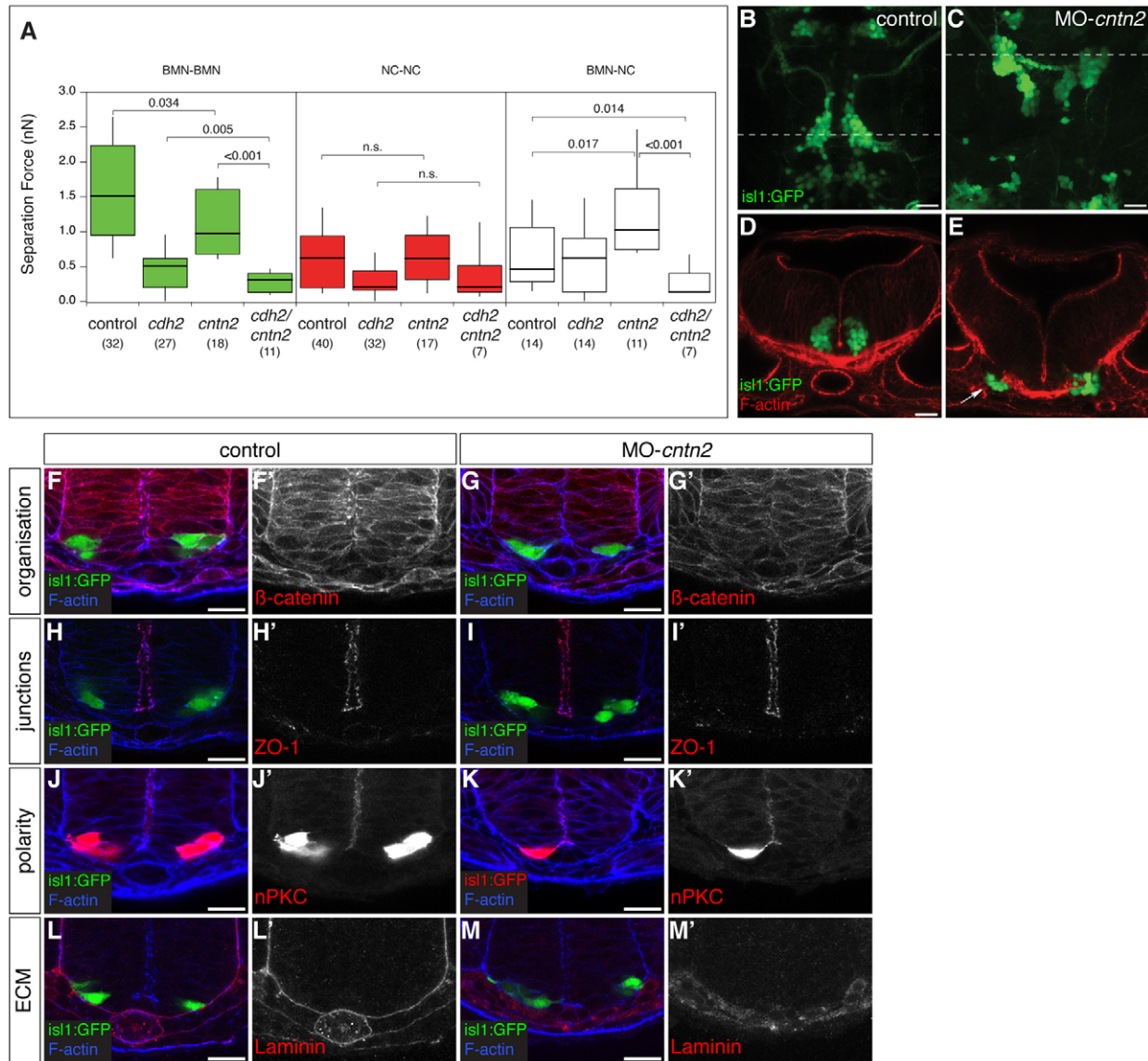


Fig. 5. *Cntn2* is required for FBMN cohesion and tangential migration. (A) Box plot of separation forces measured for homotypic adhesion between BMNs (BMN-BMN) and NCs (NC-NC), and for heterotypic adhesion between BMNs and NCs (BMN-NC) taken from control, *cdh2* mutant and *cntn2* morphant embryos, and from *cdh2* mutant embryos injected with *cntn2* MO (*cdh2/cntn2*). Box represents the median \pm interquartile range (IQR) and the whiskers extend to $1.5 \times$ IQR. *P* values determined by *t*-test are shown above the brackets. n.s., not significant. (B-E) *cntn2* morphant embryos (1.3 ng/embryo; C,E) exhibit reduced tangential FBMN migration (C) and basal extrusion of FBMNs from the neural tube at 48 hpf (white arrow in E). Dashed lines in B,C indicate level of transverse sections shown in D,E. (F-M') Confocal images of wt and *cntn2* morphant transgenic *isl1:GFP* embryos at 18 ss immunolabeled with antibodies against β -catenin (F-G'), tight junction protein ZO-1 (H-I'), apical protein nPKC (J-K') and extracellular matrix component Laminin (L-M'). Scale bars: 20 μ m.

the *cdh2* FBMN migration phenotype, we performed high-resolution movies of FBMN movements in double mutant/morphant embryos (Fig. 6E-G; see Movie 7 in the supplementary material). *Cdh2/cntn2* double mutant/morphant embryos showed phenotypic aspects characteristic for the single mutant/morphant phenotypes, such as a disorganized dorsal neural tube, diminished basal lamina formation and reduced tangential FBMN movements (Fig. 5C; data not shown). Moreover, the general architecture of the ventral neural tube, where FBMNs are specified and migrate, appeared to be largely unaffected in *cdh2/cntn2* double mutant/morphant embryos (see Fig. S5 in the supplementary material), similar to the situation in single

mutant/morphant embryos. In contrast to these additive effects in the double mutant/morphant embryos, the midline fusion of the bilateral FBMN clusters in *cdh2* single mutants was partially normalized at the 22 ss by the injection of *cntn2* MO in *cdh2* mutant embryos (Fig. 6I). This was caused by FBMNs in *cdh2/cntn2* embryos initially moving apically toward the neural tube midline, but then failing to establish firm contacts over the apical midline (Fig. 6E-G; see Movie 7 in the supplementary material). These findings suggest that FBMN cohesion and/or FBMN-to-NC adhesion do not modulate the activity of NC cohesion in restricting apical FBMN movements, but do diminish FBMN cluster fusion in embryos with reduced NC cohesion.

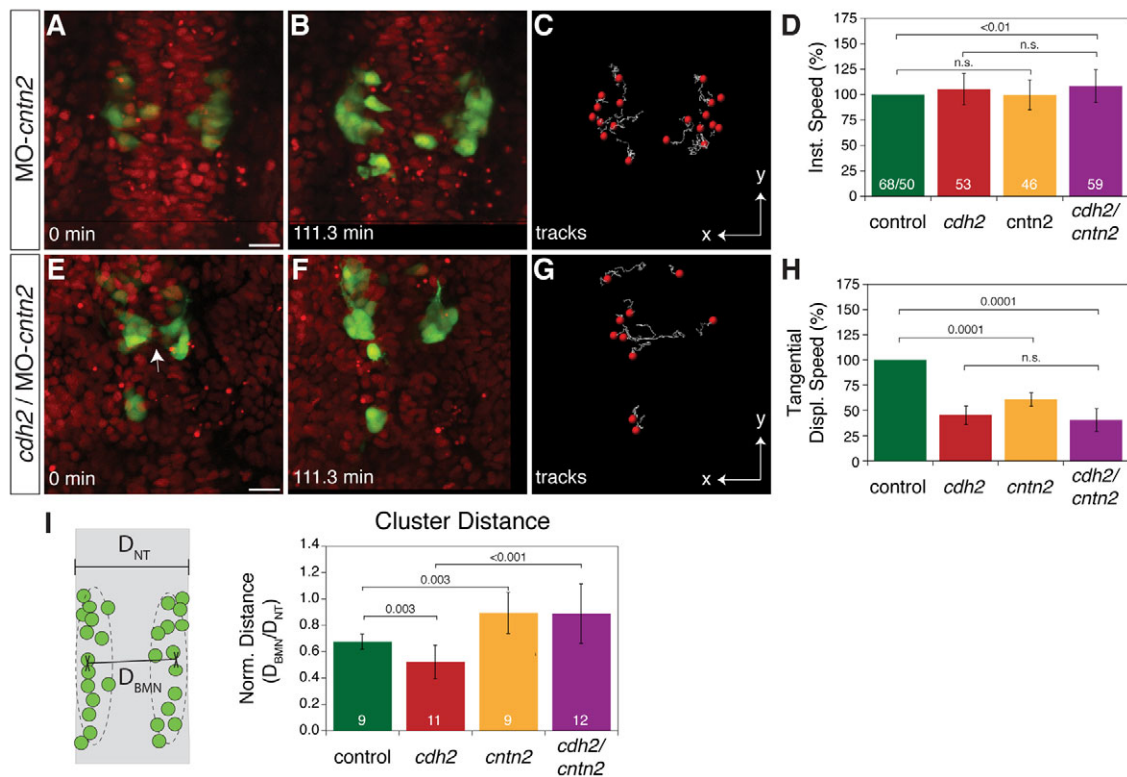


Fig. 6. Cntn2-mediated FBMN cohesion is required for apical FBMN cluster fusion in *cdh2* mutants. (A-C,E-G) Live imaging of FBMN migration in *cntn2* morphant and *cdh2* mutant embryos injected with *cntn2*-MO starting at 18 ss. (D,H) Average instantaneous (D) and tangential displacement (H) speed of FBMN movements in *cdh2* mutant, *cntn2* morphant and *cdh2/cntn2* mutant/morphant embryos, normalized to their respective controls. Mean values \pm s.d. (D) and mean \pm s.e.m. (H) are shown. (I) Normalized FBMN cluster distance in *cdh2* mutant, *cntn2* morphant and *cdh2/cntn2* mutant/morphant embryos (mean values \pm s.d.). *P* values determined by *t*-test are shown above the brackets. Scale bars: 20 μ m.

DISCUSSION

Here, we have tested the hypothesis that cohesion among NCs is required for FBMN migration by restricting apical movement of FBMNs within the neuroepithelium. We show that lowering NC cohesion causes FBMNs positioned at the basal side of the neuroepithelium to move apically instead of tangentially towards r6/7. NC cohesion, controlled by the Wnt/PCP signaling pathway, has previously been suggested to prevent FBMNs from moving apically between NCs, and ectopic apical FBMN movement has been associated with failed tangential FBMN migration in Wnt/PCP mutant embryos (Wada et al., 2006). Our data now provide direct experimental evidence in favor of the hypothesis that NC cohesion functions in tangential FBMN migration by restricting apical FBMN movement.

FBMNs migrate tangentially in close proximity to the outer (basal or pial) surface of the hindbrain epithelium and form protrusions pointing in the direction of their migration (see Movie 8 in the supplementary material). They also frequently form protrusions pointing apically between NCs (Mapp et al., 2010), but in embryos with normal NC cohesion, these projections are only short-lived and do not lead to apical translocation of FBMNs (see Movie 8 in the supplementary material, red arrows). It is therefore likely that FBMNs use NCs as a substrate for their migration, and that the path of their migration is, at least partially, determined by the cohesive properties of their substrate. Consequently, in embryos with normal NC cohesion (wt embryos), FBMNs migrate tangentially and not apically, as moving between NCs would be

mechanically unfavorable. By contrast, when NC cohesion is low (*cdh2* mutants), FBMNs move apically instead of tangentially, as there is no sufficient mechanical resistance from the neuroepithelium to restrict their apical movement. A similar situation might exist in *Drosophila* oogenesis; border cells fail to migrate when E-cadherin expression is reduced in nurse cells, which border cells use as their substrate for migration (Niewiadomska et al., 1999). Although the cohesive function of E-cadherin in nurse cells has not yet been tested directly, it is conceivable that reduced E-cadherin expression leads to diminished nurse cell cohesion, and that sufficient nurse cell cohesion is required for directed border cell migration.

Cell-to-substrate adhesion is thought to be crucial for cell migration in various developmental processes, such as border cell migration in *Drosophila* (Pacquelet and Rorth, 2005), mesoderm migration in *Xenopus* and zebrafish (Winklbauer et al., 1992; Montero et al., 2005), and primordial germ cell migration in zebrafish (Kardash et al., 2010). Given that FBMNs are likely to use the outer surface of the hindbrain as a substrate for their migration (Grant and Moens, 2010), heterotypic adhesion between FBMNs and NCs will also be an important factor influencing their migration. Our finding that reduced homotypic FBMN and NC adhesion but unchanged heterotypic FBMN-to-NC adhesion in *cdh2* mutant embryos is accompanied by ectopic apical FBMN movements (Figs 2 and 4), argues against a major function of heterotypic adhesion in causing apical instead of tangential FBMN movements in *cdh2* mutants. However, it is conceivable that

heterotypic adhesion has other functions in FBMN migration, such as the regulation of FBMN traction required for efficient translocation of FBMNs over NCs. Our observation that in *cntn2* morphant embryos increased FBMN-to-NC adhesion (and reduced FBMN cohesion) is accompanied by failed tangential FBMN migration (Figs 5 and 6), indicates a possible involvement of heterotypic adhesion in FBMN migration.

Cdh2 has previously been shown to be required for neuroepithelial morphogenesis in zebrafish (Lele et al., 2002). In *cdh2* mutant embryos, NC movements are affected and neurons become progressively displaced during neural tube formation. These phenotypes are particularly pronounced in dorsal regions of the midbrain and hindbrain, whereas other parts of the neural tube are less affected. Our finding that NC cohesion is nearly completely abolished in *cdh2* mutant embryos (Fig. 2), whereas the architecture of the ventral neuroepithelium appears to be normal (Fig. 3), suggests that Cdh2-dependent NC cohesion is largely dispensable for maintaining epithelial organization in ventral parts of the neural tube. However, once epithelial integrity is challenged, e.g. by basally positioned FBMNs trying to squeeze between NCs (Mapp et al., 2010), reduced neuroepithelial stability in *cdh2* mutants becomes apparent by the apical dislocation of FBMNs.

Cdh2 is expressed in both NCs and FBMNs and is required for cohesion of both cell types (Fig. 2). Our observation that reduced cohesion of FBMNs in *cntn2* mutant embryos does not lead to ectopic apical FBMN movement, as observed in *cdh2* mutants (Figs 5 and 6), argues against a crucial function of Cdh2 in controlling apical FBMN movements by regulating FBMN cohesion. However, it is still possible that Cdh2 functions differently in FBMNs to control their migration. To address such potential Cdh2 function in FBMNs, we have performed cell transplantation experiments, in which we transplanted either mutant cells into wt embryos or vice versa to examine a cell-autonomous function of Cdh2 in either FBMNs or NCs. However, wt cells transplanted into *cdh2* mutant hindbrains, and mutant cells transplanted into wt hindbrains, often formed clones clearly segregated from the surrounding neuroepithelium (data not shown), rendering these transplantation experiments uninterpretable. We can therefore presently not exclude that Cdh2 also functions in FBMNs to control their migration independently from regulating their cohesion.

The regulation of homotypic and heterotypic cell adhesion within the developing neural tube is likely to be controlled by a variety of different adhesion molecules. Our analysis of *cdh2* and *cntn2* mutant/morphant embryos revealed that Cdh2 is required for most of NC cohesion, whereas FBMN cohesion requires the cooperative activities of Cdh2 and Cntn2 (Figs 2 and 5). Interestingly, NC-to-FBMN adhesion is unaffected in *cdh2* mutants (Fig. 2), and is even upregulated in *cntn2* morphant embryos (Fig. 5), suggesting that heterotypic adhesion is largely independent of Cdh2 expression, and that Cntn2 has some antagonistic activity in regulating this adhesion. How Cdh2 and Cntn2 functionally interact to regulate heterotypic NC-to-FBMN adhesion, and whether other adhesion molecules are also involved, remains to be elucidated.

Neuronal migration is generally thought to be controlled by a number of evolutionarily conserved ligand-receptor systems mediating chemotaxis and contact guidance (Rao et al., 2002). Our finding that cell cohesion-mediated mechanical stability of the neuroepithelium is required to restrict the movement of FBMNs towards the apical midline of the neural tube suggests that, in addition to molecular guidance cues, the mechanical property of adjacent tissues constitute a crucial factor in neuronal migration.

Future studies will be needed to address how molecular and mechanical guidance cues interact in order to control neuronal migration in development.

Acknowledgements

We thank C. Moens and J. Geiger for critical reading of earlier versions of this manuscript and members of the Heisenberg laboratory for discussions. We are grateful to the microscopy facility of the MPI-CBG and IST Austria for continuous support; I. Nüsslein, J. Compagnon and Alex Eichner for help with cell sorting; and the fish facility of the MPI-CBG and IST Austria for excellent fish care.

Funding

This work was supported by a PhD fellowship from the Austrian Academy of Sciences to P.S. and grants/funds from the Deutsche Forschungsgemeinschaft (DFG), the Max-Planck-Gesellschaft (MPG) and the Institute of Science and Technology (IST) Austria to C.-P.H.

Competing interests statement

The authors declare no competing financial interests.

Supplementary material

Supplementary material for this article is available at <http://dev.biologists.org/lookup/suppl/doi:10.1242/dev.071233/-/DC1>

References

- Bingham, S., Higashijima, S.-i., Okamoto, H. and Chandrasekhar, A. (2002). The Zebrafish trilobite gene is essential for tangential migration of branchiomotor neurons. *Dev. Biol.* **242**, 149-160.
- Carreira-Barbosa, F., Concha, M. L., Takeuchi, M., Ueno, N., Wilson, S. W. and Tada, M. (2003). Prickle 1 regulates cell movements during gastrulation and neuronal migration in zebrafish. *Development* **130**, 4037-4046.
- Chandrasekhar, A., Moens, C. B., Warren, J. T., Kimmel, C. B. and Kuwada, J. Y. (1997). Development of branchiomotor neurons in zebrafish. *Development* **124**, 2633-2644.
- Daoudi, M., Lavergne, E., Garin, A., Tarantino, N., Debré, P., Pincet, F., Combadière, C. and Deterre, P. (2004). Enhanced adhesive capacities of the naturally occurring Ile249-Met280 variant of the chemokine receptor CX3CR1. *J. Biol. Chem.* **279**, 19649-19657.
- Denaxa, M., Chan, C. H., Schachner, M., Parnavelas, J. G. and Karagozeos, D. (2001). The adhesion molecule TAG-1 mediates the migration of cortical interneurons from the ganglionic eminence along the corticofugal fiber system. *Development* **128**, 4635-4644.
- Grant, P. K. and Moens, C. B. (2010). The neuroepithelial basement membrane serves as a boundary and a substrate for neuron migration in the zebrafish hindbrain. *Neural Dev.* **5**, 9.
- Harrington, M. J., Hong, E., Fasanmi, O. and Brewster, R. (2007). Cadherin-mediated adhesion regulates posterior body formation. *BMC Dev. Biol.* **7**, 130.
- Higashijima, S., Hotta, Y. and Okamoto, H. (2000). Visualization of cranial motor neurons in live transgenic zebrafish expressing green fluorescent protein under the control of the islet-1 promoter/enhancer. *J. Neurosci.* **20**, 206-218.
- Jessen, J. R., Topczewski, J., Bingham, S., Sepich, D. S., Marlow, F., Chandrasekhar, A. and Solnica-Krezel, L. (2002). Zebrafish trilobite identifies new roles for Strabismus in gastrulation and neuronal movements. *Nat. Cell Biol.* **4**, 610-615.
- Jontes, J. D., Emond, M. R. and Smith, S. J. (2004). In vivo trafficking and targeting of N-cadherin to nascent presynaptic terminals. *J. Neurosci.* **24**, 9027-9034.
- Kardash, E., Reichman-Fried, M., Maitre, J. L., Boldajipour, B., Papusheva, E., Messerschmidt, E. M., Heisenberg, C. P. and Raz, E. (2010). A role for Rho GTPases and cell-cell adhesion in single-cell motility in vivo. *Nat. Cell Biol.* **12**, 47-53.
- Kawauchi, T., Sekine, K., Shikanai, M., Chihama, K., Tomita, K., Kubo, K.-i., Nakajima, K., Nabeshima, Y.-i. and Hoshino, M. (2010). Rab GTPases-dependent endocytic pathways regulate neuronal migration and maturation through N-cadherin trafficking. *Neuron* **67**, 588-602.
- Kimmel, C. B., Ballard, W. W., Kimmel, S. R., Ullmann, B. and Schilling, T. F. (1995). Stages of embryonic development of the zebrafish. *Dev. Dyn.* **203**, 253-310.
- Kyriakopoulou, K., de Diego, I., Wassef, M. and Karagozeos, D. (2002). A combination of chain and neurophilic migration involving the adhesion molecule TAG-1 in the caudal medulla. *Development* **129**, 287-296.
- Lele, Z., Folchert, A., Concha, M., Rauch, G.-J., Geisler, R., Rosa, F., Wilson, S. W., Hammerschmidt, M. and Bally-Cuif, L. (2002). parachute/n-cadherin is required for morphogenesis and maintained integrity of the zebrafish neural tube. *Development* **129**, 3281-3294.

- Liu, Y. and Halloran, M. C. (2005). Central and peripheral axon branches from one neuron are guided differentially by Semaphorin3D and transient axonal glycoprotein-1. *J. Neurosci.* **25**, 10556-10563.
- Maness, P. F. and Schachner, M. (2007). Neural recognition molecules of the immunoglobulin superfamily: signaling transducers of axon guidance and neuronal migration. *Nat. Neurosci.* **10**, 19-26.
- Mapp, O. M., Wanner, S. J., Rohrschneider, M. R. and Prince, V. E. (2010). Prickle1b mediates interpretation of migratory cues during zebrafish facial branchiomotor neuron migration. *Dev. Dyn.* **239**, 1596-1608.
- Montero, J.-A., Carvalho, L., Wilsch-Bräuninger, M., Kilian, B., Mustafa, C. and Heisenberg, C.-P. (2005). Shield formation at the onset of zebrafish gastrulation. *Development* **132**, 1187-1198.
- Niewiadowska, P., Godt, D. and Tepass, U. (1999). DE-Cadherin is required for intercellular motility during *Drosophila* oogenesis. *J. Cell Biol.* **144**, 533-547.
- Pacquelet, A. and Rorth, P. (2005). Regulatory mechanisms required for DE-cadherin function in cell migration and other types of adhesion. *J. Cell Biol.* **170**, 803-812.
- Rao, Y., Wong, K., Ward, M., Jurgensen, C. and Wu, J. Y. (2002). Neuronal migration and molecular conservation with leukocyte chemotaxis. *Genes Dev.* **16**, 2973-2984.
- Rieger, S., Senghaas, N., Walch, A. and Koster, R. W. (2009). Cadherin-2 controls directional chain migration of cerebellar granule neurons. *PLoS Biol.* **7**, e1000240.
- Sittaramane, V., Sawant, A., Wolman, M., Maves, L., Halloran, M. C. and Chandrasekhar, A. (2009). The cell adhesion molecule Tag1, transmembrane protein Stbm/Vangl2, and Laminin α 1 exhibit genetic interactions during migration of facial branchiomotor neurons in zebrafish. *Dev. Biol.* **325**, 363-373.
- Taniguchi, H., Kawauchi, D., Nishida, K. and Murakami, F. (2006). Classic cadherins regulate tangential migration of precerebellar neurons in the caudal hindbrain. *Development* **133**, 1923-1931.
- Wada, H., Iwasaki, M., Sato, T., Masai, I., Nishiwaki, Y., Tanaka, H., Sato, A., Nojima, Y. and Okamoto, H. (2005). Dual roles of zygotic and maternal Scribble1 in neural migration and convergent extension movements in zebrafish embryos. *Development* **132**, 2273-2285.
- Wada, H., Tanaka, H., Nakayama, S., Iwasaki, M. and Okamoto, H. (2006). Frizzled3a and Celsr2 function in the neuroepithelium to regulate migration of facial motor neurons in the developing zebrafish hindbrain. *Development* **133**, 4749-4759.
- Warren, J. T., Jr, Chandrasekhar, A., Kanki, J. P., Rangarajan, R., Furley, A. J. and Kuwada, J. Y. (1999). Molecular cloning and developmental expression of a zebrafish axonal glycoprotein similar to TAG-1. *Mech. Dev.* **80**, 197-201.
- Westerfield, M. (2000). *The Zebrafish Book: A Guide for the Laboratory Use of Zebrafish (Danio rerio)*. Eugene, OR: University of Oregon Press.
- Winklbauer, R., Selchow, A., Nagel, M. and Angres, B. (1992). Cell interaction and its role in mesoderm cell migration during *Xenopus* gastrulation. *Dev. Dyn.* **195**, 290-302.